

Electronic Supplementary Information

Quantitative Characterization of the Colloidal Stability of Metallic Nanoparticles using UV-vis Absorbance Spectroscopy

Tyler Ray, Bethany Lettiere, Joseph de Rutte, and Sumita Pennathur
Department of Mechanical Engineering, University of California, Santa Barbara
Santa Barbara, CA 93106, USA

sumita@engineering.ucsb.edu

Contents

| | |
|---|-----|
| Table S1: Nanoparticle Characterization Methods | S2 |
| Nanoparticle Properties | S3 |
| Estimation of Free-CTAB in Solution | S4 |
| Addendum to DLS / PIP Case Study (Figure 2) | S4 |
| Influence of CTAB Concentration on DLS Measurements | S5 |
| Particle Instability Parameter (PIP) Derivation | S6 |
| Full Plot of Figure 5 | S12 |
| Buffer Preparation Procedures | S13 |
| Sample Mixing Discussion | S14 |
| Expanded Plot of Figure 3 | S16 |
| Supplemental Video Description | S16 |

Table S1: Characterization Methods for NP Aggregation Analysis

| Method | Physical Measured Quantity | | Calculated Quantity | | Features | | | Limitations | Ref |
|---|--------------------------------|-----------------------------------|---------------------|----------|----------|-------------|--------------------|---|--|
| | size, shape, composition | concentration | <i>in-situ</i> | Ensemble | Dynamic | Destructive | Size Restrictions | | |
| Transmission Electron Microscopy (TEM) | size, shape, composition | concentration | N | N | N | Y | none | Solid state measurement. Better sensitivity to electron-dense materials. Measurement hampered by non-uniform distribution of particles (<i>e.g.</i> NP clumping) | 2,3 4,5 6,7 |
| Scanning Electron Microscopy (SEM) | size, shape, composition | concentration | N | N | N | Y | none | Typically solid state measurement. Best for uniform distribution of particles. | 8,9 |
| Darkfield Microscopy | optical response | size, aspect ratio, concentration | Y | N | Y | N | none | Liquid or solid state measurement. Individual particle measurements require costly objectives and experimental setup. | 10 |
| Spectroscopy: Dynamic Light Scattering | Brownian motion | size, diffusivity, polydispersity | Y | Y | Y | N | radius > 0.2 nm | spherical, monodisperse NPs yield best results. Non-spherical particles approximated as spheres causing errors. | 11 |
| Spectroscopy: Phase Amplitude Light Scattering (Zeta Potential) | electrophoretic mobility | zeta potential | Y | Y | Y | Y | radius > 1 nm | spherical, monodisperse NPs yield best results. High electric fields can affect sample. | 12,13 |
| Spectroscopy: UV-Vis Absorbance | spectral response (absorbance) | size, concentration | Y | Y | Y | N | none | Best if NP has strong extinction coefficient. Concentration measurements require calibration curve or other <i>a priori</i> information | 2,4,12,14-19 3,10,20,21 8,22 7,13 |
| Spectroscopy: Turbidity | light scattered by NP | concentration | Y | Y | Y | N | radius \geq 35nm | NP must not exhibit absorbance at detection wavelength. Accuracy lost at high NP concentrations. Not suitable for high concentrations of NPs | 23,24 |
| Spectroscopy: Nanoparticle Tracking Analysis (NTA) | Brownian motion | size, concentration | Y | N | Y | N | radius > 10 nm | | 25 |
| Analytical Ultra Centrifugation (AUC) | deposition rate | sedimentation response | Y | Y | Y | N | none | | 26 |
| Gravimetric Analysis | deposition rate | sedimentation response | Y | Y | Y | N | none | | 11 |

Selected reviews of characterization techniques: ^{25,27}

in-situ: NP measurements are in native solution
 Ensemble: averaged population measurement vs. single NP
 Dynamic: real-time measurement
 Destructive: NP suspension is irrecoverable or fundamentally changed by measurement

Nanoparticle Properties

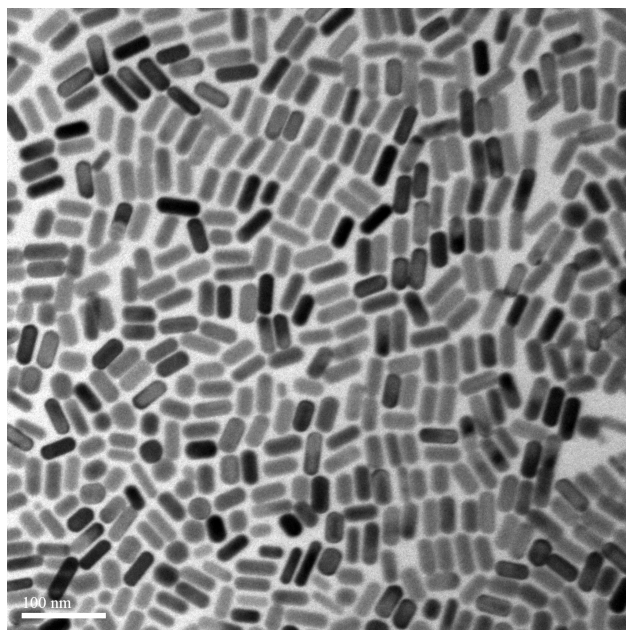


Figure S1: Transmission Electron Microscope micrograph of the AuNRs synthesized in this work. AuNR dimensions are 45 ± 8 nm \times 17 ± 4 nm as calculated from an average of 3000 nanorods.

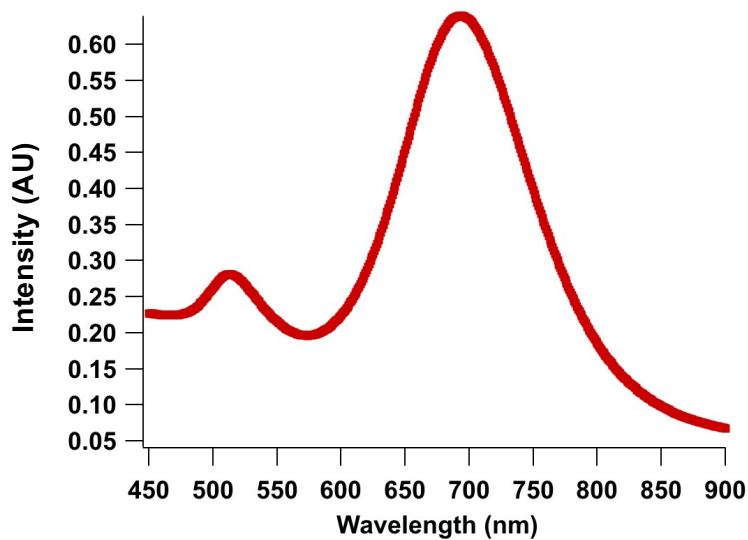


Figure S2: UV-vis Absorbance spectrum of the AuNR stock suspension used in this work. The LSPR peak is at 692 nm.

Estimation of Free-CTAB in Solution:

As the synthesized nanorods were pooled into a single stock solution, the concentration of free-CTAB was maintained as a constant throughout all experiments. We approximate that the concentration of free-CTAB in solution is 500 μM . As the CTAB concentration in the AuNR solution after synthesis is 100 mM, we purify the nanorods through a single round of centrifugation. The nanorods are extracted and resuspended in DI water with $\sim 90\%$ of the supernate removed. Thus, the CTAB concentration of the purified stock solution is ~ 10 mM CTAB. To ensure consistency, we used a 1 mL pipette set at 0.95 mL to remove the supernate after the second purification step thereby removing 95% of the supernate. Thus, the concentration of free-CTAB in the actual experimental measurements is approximately 500 μM .

Addendum to the DLS / PIP Case Study (Figure 2)

We would first note that Figure 2 is offered as a case study showcasing the performance of the PIP as compared to DLS measurements of the same colloid system, not as a systematic investigation similar to the data presented later in the manuscript. We performed a similar study of colloidal stability (in triplicate) with a different population of nanorods prepared in a similar manner to study the experimental error in the DLS measurements. We note that as a consequence the amount of free-CTAB in solution of the purified nanorods is slightly different than the solution described in the manuscript. However, the observed trend is still similar to that reported. The maximum standard deviation recorded between experiments after 15 min was 6.63 nm for the purified nanorod samples and 1.59 nm for the 1 mM CTAB samples. Included below in Table S2 are the averaged data and standard deviation from these experiments.

Table S2: Hydrodynamic radius and standard deviation from Dynamic Light Scattering measurements for AuNRs suspended in different concentrations of CTAB

| Salt Concentration (mM) | Purified AuNRs | | AuNRs resuspended in 1 mM CTAB | |
|-------------------------|--------------------------|-------------------------|--------------------------------|-------------------------|
| | Hydrodynamic Radius (nm) | Standard Deviation (nm) | Hydrodynamic Radius (nm) | Standard Deviation (nm) |
| 10 | 8.81 | 0.04 | 7.37 | 0.71 |
| 100 | 155.42 | 6.63 | 7.74 | 0.44 |
| 500 | 164.18 | 4.81 | 12.89 | 0.61 |
| 1000 | 117.80 | 4.07 | 8.12 | 1.59 |

Influence of CTAB Concentration on DLS Measurements:

We note that as seen in Table S3 below, the resuspension of AuNRs in 1 mM free-CTAB slightly increases the measured hydrodynamic radius. This results from the averaging the intensity peak associated with the AuNRs and that associated with the 1 mM CTAB. Although a regulants fit would identify these two independent peaks, the cumulants fit of the intensity signal better captures the onset and evolution of AuNR aggregation.

Table S3: Hydrodynamic radius measured by Dynamic Light Scattering for AuNRs suspended in different concentrations of CTAB

| | 1 mM CTAB without AuNRs | Purified AuNRs | AuNRs resuspended in 1 mM CTAB |
|-------------------------------------|------------------------------------|-----------------------|---|
| Hydrodynamic Radius (nm) | 2.19±0.9 | 7.18±0.11 | 10.41±0.37 |

Particle Instability Parameter (PIP) Derivation:

The PIP provides a quantitative analysis of colloidal instability using UV-vis Absorbance Spectroscopy. The development of PIP is based upon the analysis of the information available from a spectrum.

Figure S3 shows the UV-vis spectrum series of a stable (A) and unstable (B) suspension destabilized by the introduction of two different concentrations of NaBr.

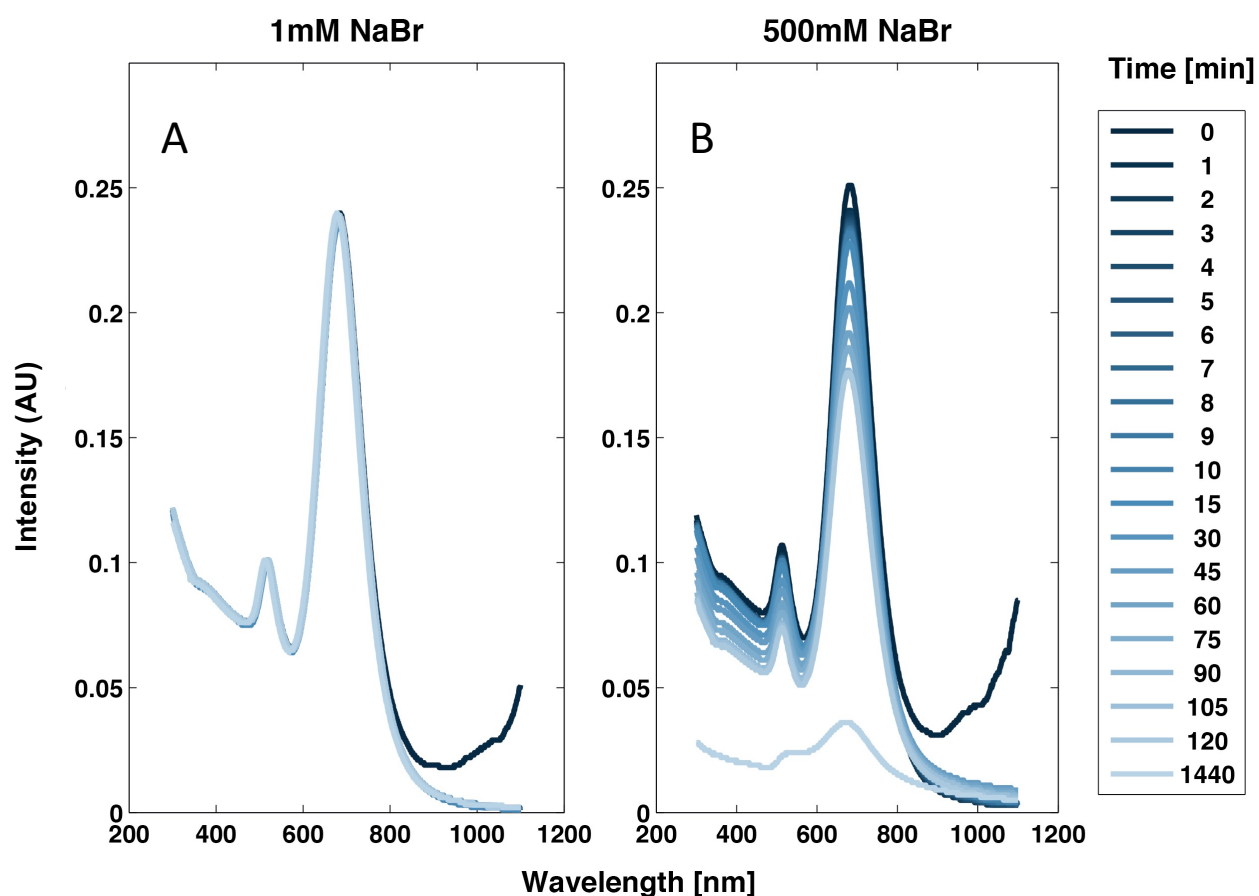


Figure S3: UV-vis Absorbance spectrum series over time of the AuNR stock suspension with (A) 1 mM NaBr and (B) 500 mM NaBr. (A) shows no variation over the time frame examined (24 h) while (B) shows a steady decrease in peak intensity for the first 2 h with a large decrease in peak intensity and large change in peak shape after 24 h.

To better understand how the components of the NP absorbance spectra are related to colloidal stability, we systematically studied how changes in peak height, peak wavelength, spectral skewness, spectral area, and derivatives of spectra described the stability of AuNRs in suspension to derive the PIP.

Figure S4 shows a plot of a spectral series. As the nanorods aggregate, the shape of the spectra changes. Although the shape (or skewness) of the spectrum changes over time as seen in Figure S5, both the peak intensity and peak wavelength position shift as well. Consequently, characterizing the spectral skewness (*e.g.* deviation from an ideal Gaussian) did not provide any additional information. Figure S6 shows a plot of a simulated spectral series versus the area of the derivative of the spectra. The area of the derivative was chosen to eliminate any differences due to changes in the spectral baseline. As seen by the two different series (with and without offset), differences in baseline are eliminated. However, if PIP uses a reference spectrum, this advantage is negated and yields a simpler assessment method. As a consequence, PIP uses only the change in peak wavelength and peak intensity to assess the degree of instability in a colloidal suspension.

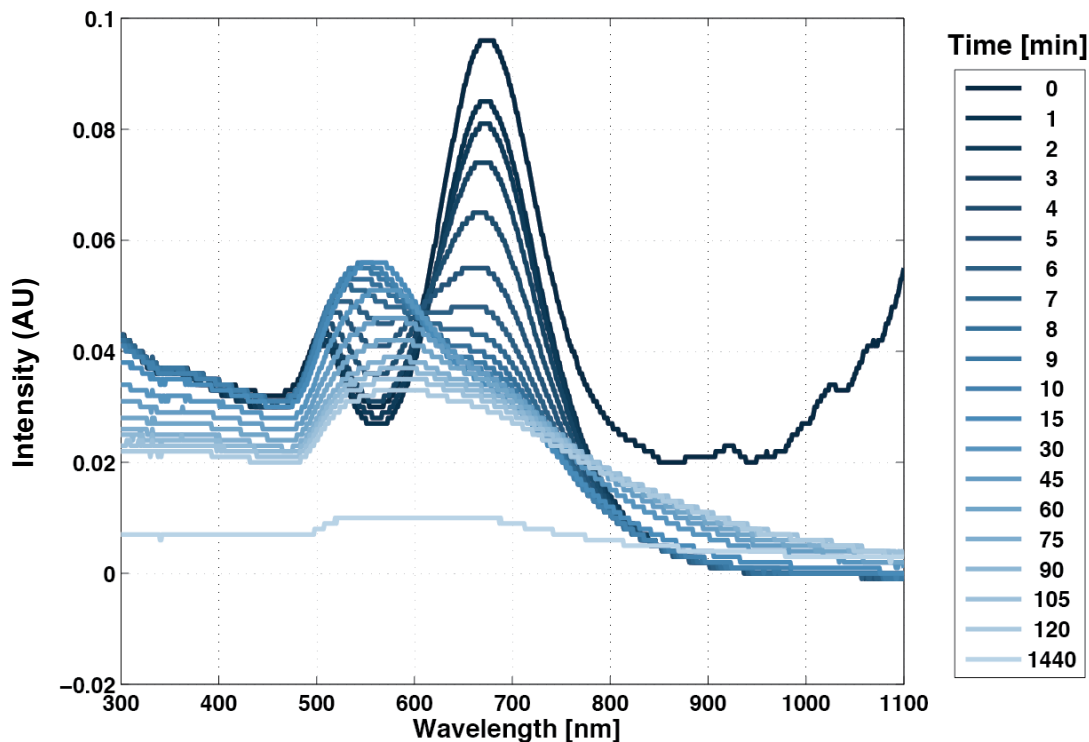


Figure S4: UV-vis Absorbance spectrum series over time of a sample AuNR stock suspension with 1 M NaCl added showing the spectral evolution of an unstable suspension.

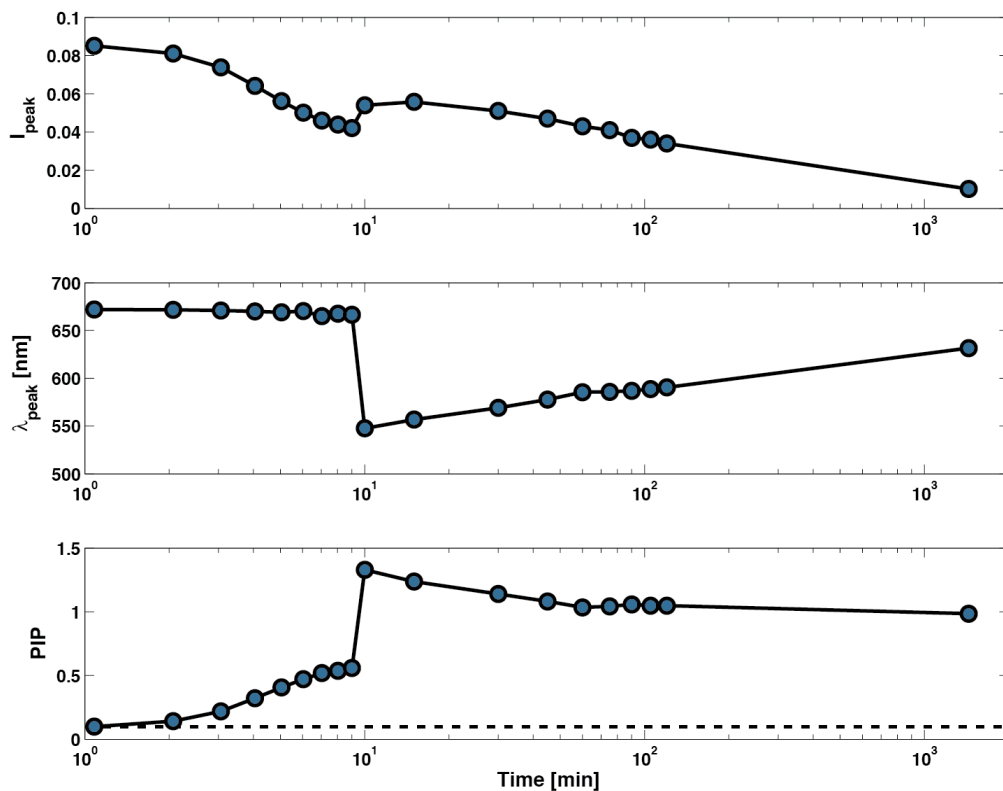


Figure S5: Comparison of the changes in peak intensity (top), peak position (middle), and PIP (bottom) from the spectra in Figure S4. PIP incorporates both the peak intensity and peak position to assess suspension instability.

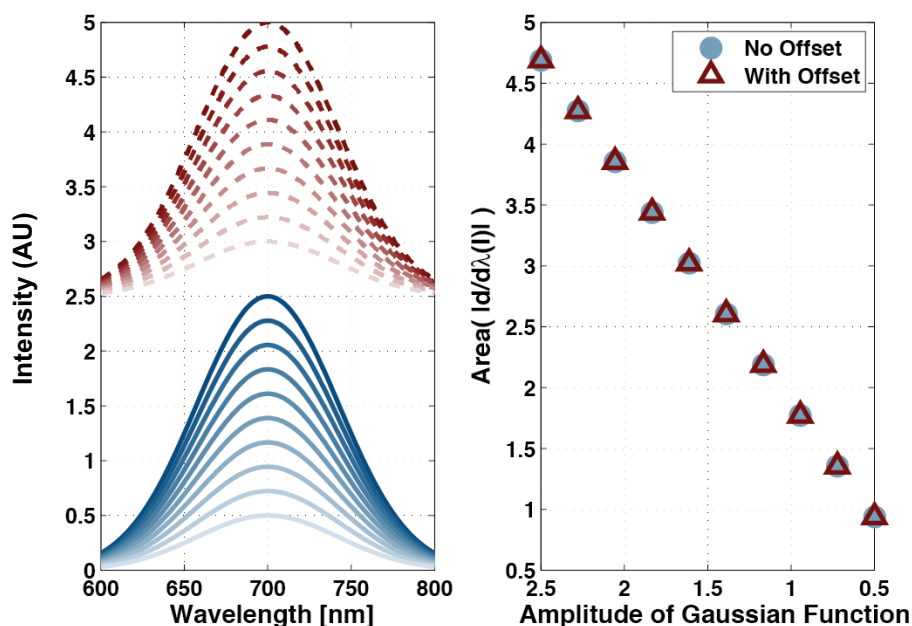


Figure S6: Sample spectra with and without a baseline offset (left) as compared with the calculated area of the derivative of the same spectra (right). By taking the derivative of the spectra, any baseline changes are ignored that could falsely indicate a change in sample stability. Taking the area of the resulting spectra, captures the aggregation behavior in the simulated spectra, which is found to be identical after removal of the baseline offset by the derivative.

Traditional techniques of qualitative colloidal analysis use control experiments to establish a baseline behavior of a system. After an experiment in which a destabilizing factor is introduced to the suspension, a separate measurement is recorded documenting the response of the colloidal suspension to that factor. These are two separate, independent measurements. We note this distinction as the PIP uses an internal reference (t_0) to compare the behavior of a colloidal suspension *within the same measurement*. This distinction enables the PIP to both incorporate and account for changes in experimental conditions such as temperature, solvent refractive index, and time which would otherwise be lost if a reference (*i.e.* control) measurement was used independent of the sample measurement. As a result, the PIP derives independent meaning as a parameter as compared to the alternative colloidal instability measurements.

For the measurements of NaCl concentration on AuNR stability using plots similar to Figure S3, we qualitatively classified the suspensions as either stable or unstable. If suspensions were difficult to classify, they were labeled as “uncertain.” Figure S7 shows these measurements classified in this way. Overlaid on Figure S7 is a bounding box that defines the limits of stability with respect to only changes in peak intensity or peak wavelength position.

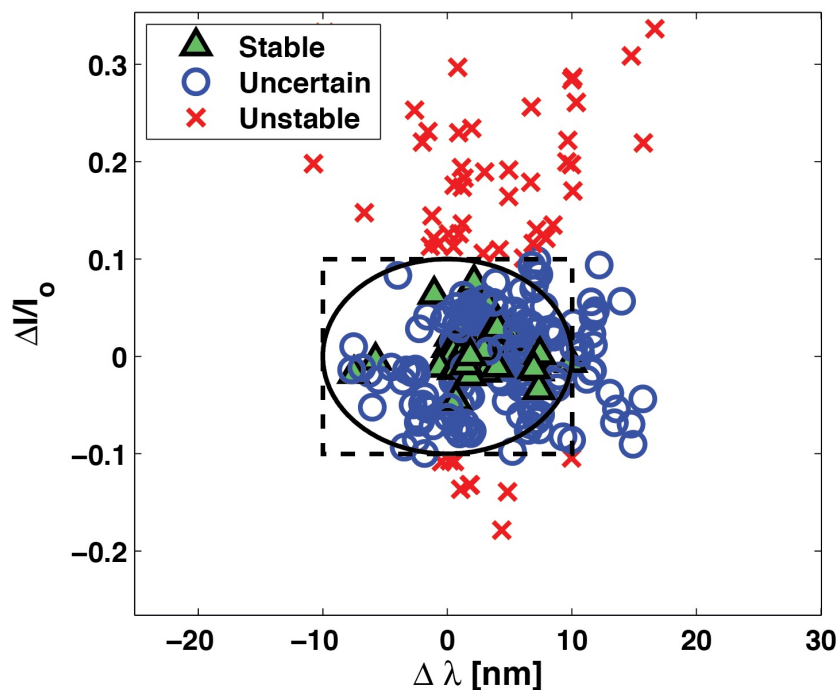


Figure S7: This scatter plot displays the all of the spectral measurements collected in this as a function of the normalized shift in peak intensity and the shift in peak wavelength. Stability assessed qualitatively based upon spectral analysis and indicated as either stable, uncertain, or unstable. The bounding box outlines a stability area defined by a limit in normalized peak intensity shift (I^*) as well as peak wavelength shift ($\Delta\lambda$). The solid ellipse is the defined PIP, which is a more conservative case where the stability zone is defined by equation (4). PIP is a quantitative analytical method to instability analysis as compared to the traditional qualitative approach of visual inspection.

As previously discussed, a suspension that experiences a change greater than 10% in intensity or a LSPR peak wavelength shift greater than 10 nm the weighted criterion is unstable. PIP includes this in its derivation such that if a suspension exhibits a change in only one criterion, PIP yields an unstable value. We note that the 10 nm cut-off value for the peak wavelength shift is selected to distinguish between a system being stable or unstable that is statistically significant outside the bounds of a signal resulting from external phenomena (*e.g.* instrument error, operator error) or slight changes to the system during a measurement (*e.g.* temperature effects). A value of 10 nm provides this significance as demonstrated both in the manuscript and the work of El-Sayed *et al*¹. When the gap between plasmonic particles (shown for different shapes) decreases (but before aggregation), the shift of the LSPR peak (scaled by the peak value) increases rapidly, typically when the physical separation distance is less than 2 nm. If the gap distance is greater than 2 nm, the LSPR wavelength shift asymptotically approaches zero. Although the gap distance at which the inflection point occurs shifts slightly with the nanoparticle shape (wavelength shift is less than 1 nm), at the particle separation distance of 2 nm, the LSPR peak wavelength shift is 10 nm. We note that although a slightly different LSPR peak wavelength shift

value could be used for a particular nanoparticle shape, 10 nm was selected to establish the PIP as a conservative, shape independent measurement method for assessing colloidal stability. As observed in Figure S7, PIP (solid ellipse) yields a more conservative measurement of instability than a stepwise function of 10% .

For the sample series in Figure S3, the PIP value is calculated for each spectrum in both the 1 mM and 500 mM NaBr set and presented in Figure S8. PIP shows the onset of instability at 15 min for the 500 mM and the relative stability of the 1 mM NaBr sample.

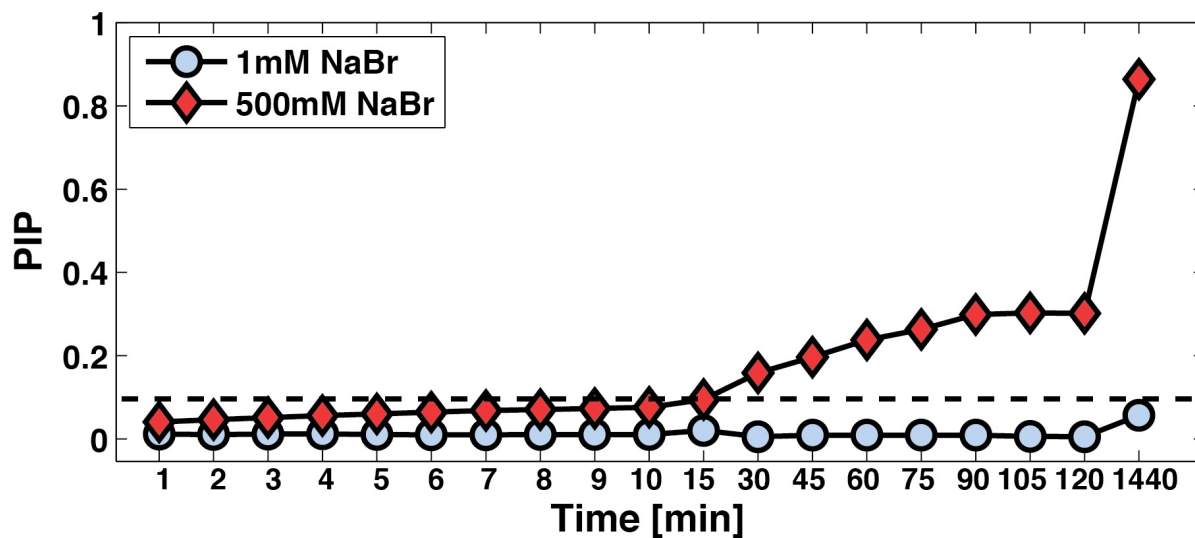


Figure S8: The calculated PIP values for AuNR suspensions with 1 mM and 500 mM NaBr added. PIP captures the onset of instability at 15 min for the 500 mM NaBr sample and the stability of the 1 mM NaBr sample over the 24 h experimental window.

Full Plot of Figure 5:

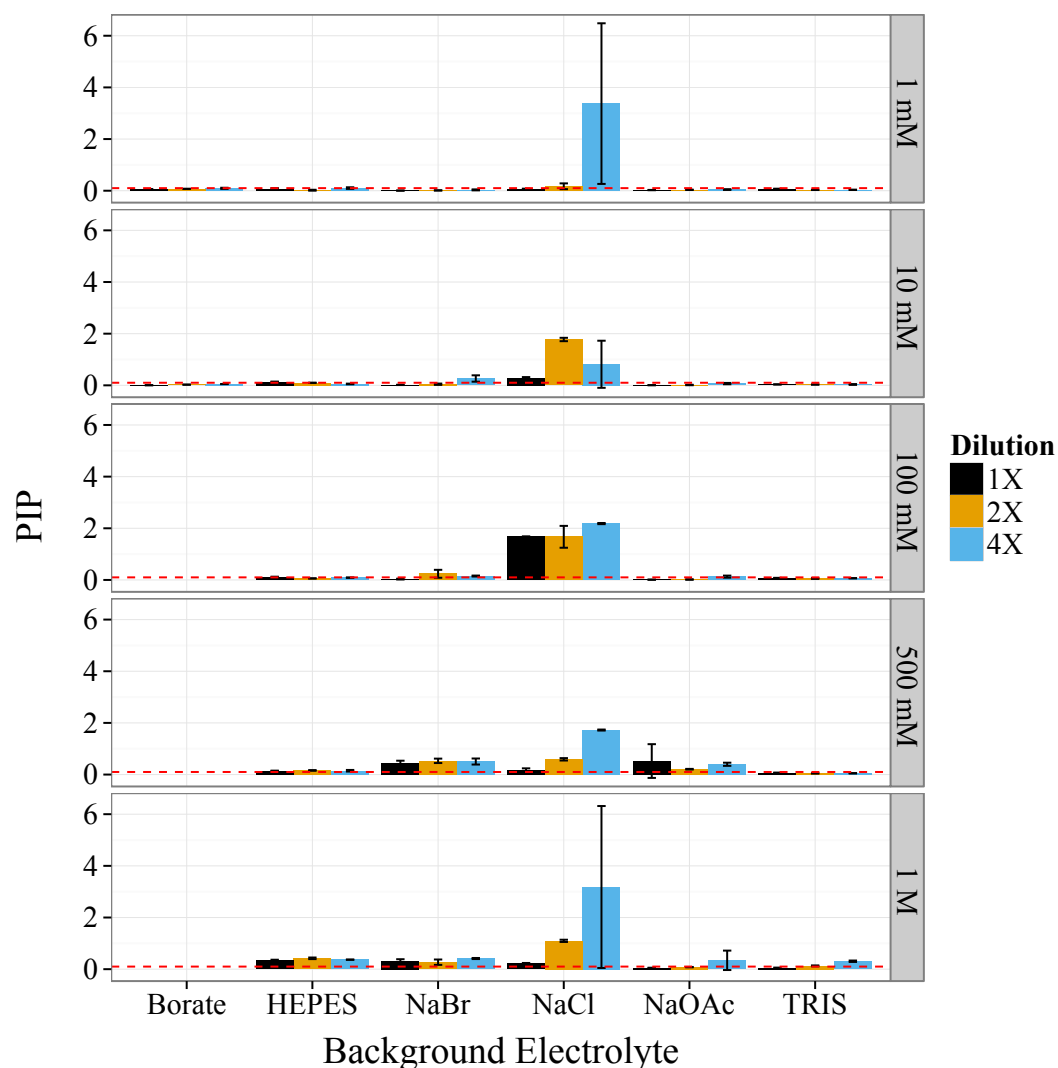


Figure S9: Bar graph comparing colloidal stability of AuNRs in response to different salts (Borate, HEPES, sodium bromide-NaBr, sodium chloride-NaCl, sodium acetate-NaOAc, and Tris) and AuNR concentration (1X, 2X, and 4X dilutions) at each salt concentration (1 mM, 10 mM, 100 mM, 500 mM, and 1 M) at 2 h. AuNR suspensions were prepared so the final analyzed AuNR concentrations were constant between salt solutions with the initial (1X) suspension serially diluted to make 2-fold (2X) and 4-fold (4X) diluted suspensions. Generally the Borate, NaBr, NaCl, and NaOAc salt solutions exhibited increased instability as AuNR concentration decreased across all salt concentrations. Exceptions include 100 mM and 1 M NaBr as well as 500 mM NaOAc. AuNR concentration only slightly influenced the AuNR suspension colloidal stability in response to HEPES and Tris across the salt concentration range studied. NaCl exhibited the most AuNR concentration dependent instability across the entire salt concentration range. Measurements were performed in triplicate.

Buffer Preparation Procedures:

NaCl Study:

A 2 M solution was prepared diluted to prepare a 1 M, 200 mM, 20 mM, and 2 mM solutions.

pH Sweep Study:

Solutions with pH ranging from 1-13 were prepared *via* the procedure described. All measurements, unless otherwise specified, were recorded at 22 °C. For pH 4+ solutions, Millipore water was stored in falcon tubes for over 24 h before diluting or preparing the solution to allow for pH stabilization.

Acids: 1 M HCl stock solution from Fisher Chemicals.

Bases: A stock solution of 2 M NaOH was prepared from NaOH solid (Fisher Chemicals).

Each pH solution was prepared via titration and allowed to stabilize for 24 h before use; pH values were re-verified after 24 h.

Buffer Preparation:

Note: the pH of each buffer solutions was adjusted using either concentrated HCl, NaOH, or glacial acetic acid to the desired pH. All bulk solutions were thoroughly mixed (~1000 rpm) for at least 30 min prior to adding the acid/base. Then, the resulting solution was mixed for an additional 30 min.

HEPES:

A 1 M of HEPES stock solution was prepared in 500 mL of DI water (119.15 g HEPES). After 30 min, the initial pH was 4.95 at 22.5 °C.

8.02 g NaOH was added to the solution while stirring vigorously. The final pH was 7.49 at 22.1 °C.

An additional 1.5 M solution was prepared (for the 1 M experiment) by adding 178.72 g HEPES to 500 mL DI water. After mixing, NaOH tablets were added as before. Final pH was 7.50 at 22.1 °C.

Tris:

A 2 M stock solution of Tris was prepared *via* adding 121.4 g TRIS Base to 500 mL DI water. The pH value was measured to be 10.10 at 22.1 °C.

Concentrated HCl was titrated to the solution while mixing the solution at 1000 rpm. After adding 26.5 mL of HCl, the final pH was 8.22 at 27.2 C. The pH after 24 h was measured to be pH = 8.33 at at 22.1 °C. With the addition of HCl, the molarity of the stock solution is now 1.89 M (1 mol Tris / 526.5 mL).

Sodium Acetate:

A stock solution of 2 M Sodium Acetate was prepared *via* the addition of 136.08 g sodium acetate to 500 mL Millipore water. The initial pH was measured to be pH 8.89 at 22.1 °C. 33 mL of glacial acetic acid was added while mixing at 1000 rpm to achieve a final pH value of 4.80 at 22.1 °C. The final molarity of the stock solution is 1.876 M.

Borate Buffer

A stock solution of 150 mM borate buffer was prepared from sodium tetraborate. The final pH value was measured to be 9.2 at 22.1 °C.

Sample Mixing Discussion:

To better understand the role the solvent exchange method has in determining stability, we studied five techniques to introduce background electrolyte defined as: Single Dose - Pipette (SD-P), Resuspend Dose Pipette (RD-P), Resuspend Dose - Vortex (RD-V), Dropwise Addition - Pipette (D-P), Dropwise Addition - Vortex (D-V). The techniques include three ways to add salt to a purified AuNR sample (by centrifugation), and two mixing techniques (pipette mixing-P or vortexing-V). The dosing methods are either a direct addition (Single Dose-SD) of the background electrolyte at full concentration; the resuspension of the purified AuNRs into DI water with the addition of the appropriate amount of electrolyte to bring to desired final concentration (Resuspend Dose-RD); and a dropwise addition (D) of the background electrolyte to a resuspended sample of purified AuNRs in DI water as a serial addition over time (of 50 μ L at 5 min intervals). Using different concentrations of salt solution as the background electrolyte, we characterized the time-response colloidal stability of AuNRs with PIP shown in Figure S10. This figure shows how different methods to introduce background electrolyte can influence the stability of an AuNR colloid system. We observe that RD-V is the method that least influences the stability as compared to other mixing and sample introduction methods. We note that for brevity, the PIP values shown are for sample data 15 min after analyte introduction as little difference exists between this and data from 2 or 24 h. Mixing by pipette tends to induce aggregation as compared to the stability of suspensions mixed using a vortex mixer at the same salt conditions and independent of addition method (as a single dose or serial addition). Furthermore, mixing by pipette yielded inconsistent results between AuNR aliquots for the same salt concentration while the use of a vortex mixer produced repeatable measurements across a wide range of conditions. Only at high ionic strength was AuNR aggregation observed when the analyte was added via direct addition with vortex mixing. We hypothesize that the aggregation observed when the suspension is mixed via pipette is a result of local concentration of the AuNRs as compared to the bulk suspension thereby inducing aggregation. Specifically, the pipette tip generates nucleation points for the cascade of colloidal aggregation in the system. This hypothesis is supported by the lack of aggregation observed when using a vortex mixer to well-mix the sample after the direct addition of an analyte. The possible interaction or attraction of AuNRs in suspension to the pipette tip as a result of pipette tip material composition or presence of a surface charge could also contribute to the aggregation behavior observed.

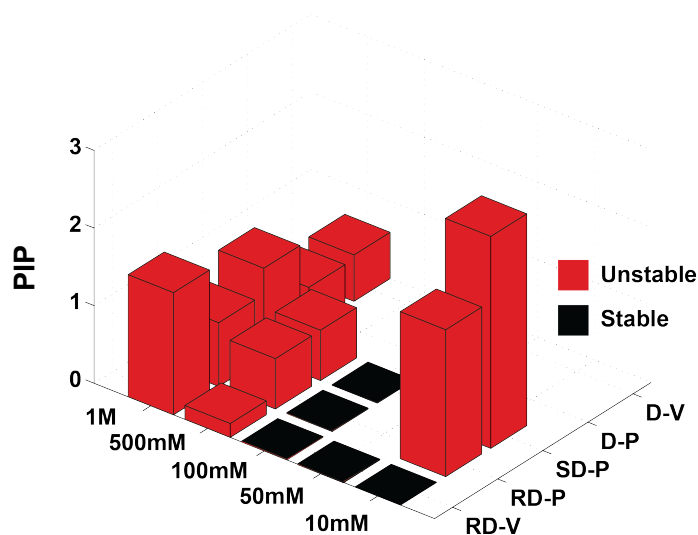


Figure S10: Bar graph comparing colloidal stability of AuNRs in response to different NaCl salt concentrations versus sample dosing technique. Five techniques to introduce background electrolyte defined as: Single Dose–Pipette (SD–P), Resuspend Dose–Pipette (RD–P), Resuspend Dose–Vortex (RD–V), Dropwise Addition–Pipette (D–P), Dropwise Addition–Vortex (D–V). The techniques include three ways to add salt to a purified AuNR sample (by centrifugation), and two mixing techniques (pipette mixing–P or vortexing–V). We observe that RD–V is the method that least influences the stability as compared to other mixing and sample introduction methods. We note that for brevity, the PIP values shown are for sample data 15 min after analyte introduction as little difference exists between this and data from 2 or 24 h. Mixing by pipette tends to induce aggregation as compared to the stability of suspensions mixed using a vortex mixer at the same salt conditions and independent of addition method (as a single dose or serial addition). Furthermore, mixing by pipette yielded inconsistent results between AuNR aliquots for the same salt concentration while the use of a vortex mixer produced repeatable measurements across a wide range of conditions. Only at high ionic strength was AuNR aggregation observed when the analyte was added via direct addition with vortex mixing.

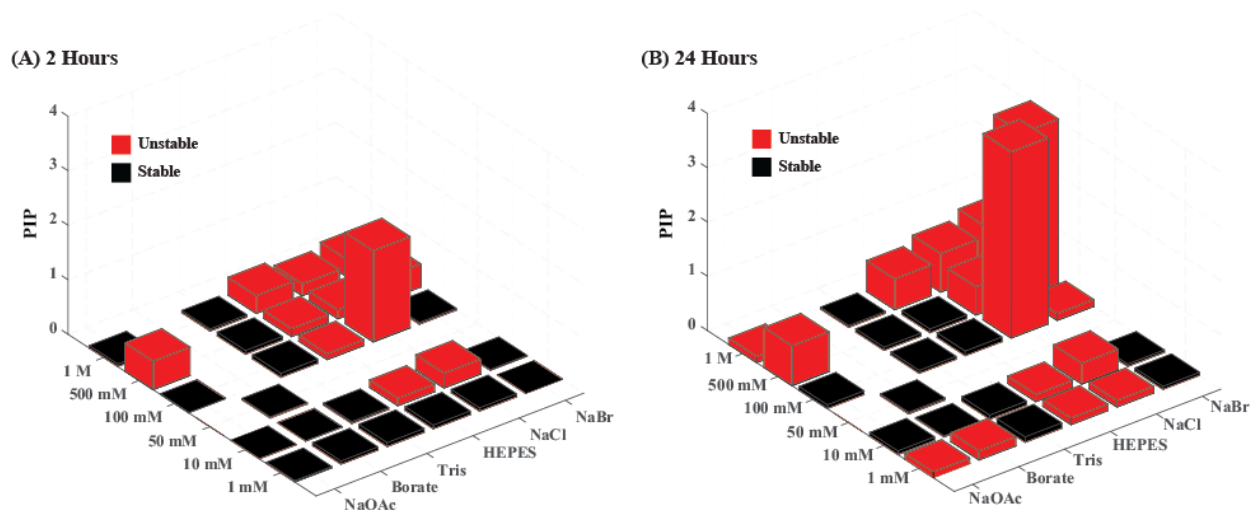


Figure S11: Stability bar graph of AuNRs in response to different salts (sodium acetate-NaOAc, borate, Tris, HEPES, sodium chloride-NaCl, and sodium bromide-NaBr) and different concentrations (1 mM, 10 mM, 50 mM, 100 mM, 500 mM, and 1 M) at 2 h (A) and 24 h (B) intervals. This chart shows the parameter space as a function of PIP with unstable values (PIP > 0.1) indicated as red. A suspension of twice-centrifuged AuNRs served as the starting suspension for all measurements and we performed each measurement in triplicate. We observe that AuNRs suspended in Tris were stable across all concentrations examined, while NaCl was unstable across all concentrations after 24 h. NaBr and NaOAc became unstable at higher salt concentrations and borate buffer was unstable after 24 h, but not at 2 h. Absence of data for borate buffer above 100 mM is due to the insolubility of sodium tetraborate in water at these concentrations.

Supplemental Video Description:

The video included with the SI shows the change in color observed upon the addition of a 1 M NaCl solution to an AuNR suspension in DI water in real-time. Frames from this video appear in the TOC Graphic for this work.

References

- (1) Tabor, C.; Murali, R.; Mahmoud, M.; El-Sayed, M. A. On the Use of Plasmonic Nanoparticle Pairs As a Plasmon Ruler: The Dependence of the Near-Field Dipole Plasmon Coupling on Nanoparticle Size and Shape. *The Journal of Physical Chemistry A* **2009**, *113*, 1946–1953, PMID: 19090688.
- (2) Merrill, N. A.; Sethi, M.; Knecht, M. R. Structural and Equilibrium Effects of the Surface Passivant on the Stability of Au Nanorods. *ACS Appl. Mater. Interfaces* **2013**, *5*, 7906–7914.
- (3) Ding, H.; Yong, K. T.; Roy, I.; Pudavar, H. E.; Law, W. C.; Bergey, E. J.; Prasad, P. N. Gold Nanorods Coated with Multilayer Polyelectrolyte as Contrast Agents for Multimodal Imaging. *J. Phys. Chem. C* **2007**, *111*, 12552–12557.
- (4) Bogliotti, N.; Oberleitner, B.; Di-Cicco, A.; Schmidt, F.; Florent, J.-C.; Semetey, V. Optimizing the Formation of Biocompatible Gold Nanorods for Cancer Research: Functionalization, Stabilization and Purification. *J. Colloid Interface Sci.* **2011**, *357*, 75–81.
- (5) Nikoobakht, B.; Wang, Z. L.; El-Sayed, M. A. Self-Assembly of Gold Nanorods. *J. Phys. Chem. B* **2000**, *104*, 8635–8640.
- (6) Orendorff, C. J.; Hankins, P. L.; Murphy, C. J. pH-Triggered Assembly of Gold Nanorods. *Langmuir* **2005**, *21*, 2022–2026.
- (7) Sethi, M.; Pacardo, D. B.; Knecht, M. R. Biological Surface Effects of Metallic Nanomaterials for Applications in Assembly and Catalysis. *Langmuir* **2010**, *26*, 15121–15134.
- (8) Guo, Z.; Fan, X.; Xu, L.; Lu, X.; Gu, C.; Bian, Z.; Gu, N.; Zhang, J.; Yang, D. Shape Separation of Colloidal Gold Nanoparticles Through Salt-Triggered Selective Precipitation. *Chem. Commun.* **2011**, *47*, 4180–4182.

- (9) Das, M.; Mordoukhovski, L.; Kumacheva, E. Sequestering Gold Nanorods by Polymer Microgels. *Adv. Mater.* **2008**, *20*, 2371–2375.
- (10) Zhan, Q.; Qian, J.; Li, X.; He, S. A Study of Mesoporous Silica-Encapsulated Gold Nanorods as Enhanced Light Scattering Probes for Cancer Cell Imaging. *Nanotechnology* **2009**, *21*, 055704.
- (11) Afrooz, A. R. M. N.; Sivalapalan, S. T.; Murphy, C. J.; Hussain, S. M.; Schlager, J. J.; Saleh, N. B. Spheres vs. Rods: The Shape of Gold Nanoparticles Influences Aggregation and Deposition Behavior. *Chemosphere* **2013**, *91*, 93–98.
- (12) Sethi, M.; Joung, G.; Knecht, M. R. Stability and Electrostatic Assembly of Au Nanorods for Use in Biological Assays. *Langmuir* **2009**, *25*, 317–325.
- (13) Kim, T.; Lee, C.-H.; Joo, S.-W.; Lee, K. Kinetics of Gold Nanoparticle Aggregation: Experiments and Modeling. *J. Colloid Interface Sci.* **2008**, *318*, 238 – 243.
- (14) Kah, J. C. Y.; Zubietta, A.; Saavedra, R. A.; Hamad-Schifferli, K. Stability of Gold Nanorods Passivated with Amphiphilic Ligands. *Langmuir* **2012**, *28*, 8834–8844.
- (15) Rostro-Kohanloo, B. C.; Bickford, L. R.; Payne, C. M.; Day, E. S.; Anderson, L. J. E.; Zhong, M.; Lee, S.; Mayer, K. M.; Zal, T.; Adam, L.; Dinney, C. P. N.; Drezek, R. A.; West, J. L.; Hafner, J. H. The Stabilization and Targeting of Surfactant-Synthesized Gold Nanorods. *Nanotechnology* **2009**, *20*, 434005.
- (16) Becker, R.; Liedberg, B.; Käll, P.-O. CTAB Promoted Synthesis of Au Nanorods – Temperature Effects and Stability Considerations. *J. Colloid Interface Sci.* **2010**, *343*, 25–30.
- (17) Ferhan, A. R.; Guo, L.; Kim, D.-H. Influence of Ionic Strength and Surfactant Concentration on Electrostatic Surface Assembly of Cetyltrimethylammonium Bromide-Capped Gold Nanorods on Fully Immersed Glass. *Langmuir* **2010**, *26*, 12433–12442.

- (18) Leonov, A. P.; Zheng, J.; Clogston, J. D.; Stern, S. T.; Patri, A. K.; Wei, A. Detoxification of Gold Nanorods by Treatment with Polystyrenesulfonate. *ACS Nano* **2008**, *2*, 2481–2488.
- (19) Tiwari, N.; Kalele, S.; Kulkarni, S. K. Modulation of Optical Properties of Gold Nanorods on Addition of KOH. *Plasmonics* **2007**, *2*, 231–236.
- (20) Alkilany, A. M.; Thompson, L. B.; Murphy, C. J. Polyelectrolyte Coating Provides a Facile Route to Suspend Gold Nanorods in Polar Organic Solvents and Hydrophobic Polymers. *ACS Appl. Mater. Interfaces* **2010**, *2*, 3417–3421.
- (21) Sethi, M.; Joung, G.; Knecht, M. R. Linear Assembly of Au Nanorods Using Biomimetic Ligands. *Langmuir* **2009**, *25*, 1572–1581.
- (22) Huang, H.-C.; Barua, S.; Kay, D. B.; Rege, K. Simultaneous Enhancement of Photothermal Stability and Gene Delivery Efficacy of Gold Nanorods Using Polyelectrolytes. *ACS Nano* **2009**, *3*, 2941–2952.
- (23) Rahn-Chique, K.; Puertas, A. M.; Romero-Cano, M. S.; Rojas, C.; Urbina-Villalba, G. Nanoemulsion Stability: Experimental Evaluation of the Flocculation Rate from Turbidity measurements. *Adv. Colloid Interface Sci.* **2012**, *178*, 1–20.
- (24) Gregory, J. Monitoring Particle Aggregation Processes. *Adv. Colloid Interface Sci.* **2009**, *147-148*, 109–123.
- (25) Shang, J.; Gao, X. Nanoparticle Counting: Towards Accurate Determination of the Molar Concentration. *Chem. Soc. Rev.* **2014**, 1–12.
- (26) Walter, J.; Löhr, K.; Karabudak, E.; Reis, W.; Mikhael, J.; Peukert, W.; Wohlleben, W.; Cölfen, H. Multidimensional Analysis of Nanoparticles with Highly Disperse Properties Using Multiwavelength Analytical Ultracentrifugation. *ACS Nano* **2014**, *8*, 8871–8886.

- (27) Mahl, D.; Diendorf, J.; Meyer-Zaika, W.; Epple, M. Possibilities and Limitations of Different Analytical Methods for the Size Determination of a Bimodal Dispersion of Metallic Nanoparticles. *Colloids Surf., A* **2011**, *377*, 386–392.